

Emission and Immunity Standards: Replacing Field-at-a-Distance Measurements with Total-Radiated-Power Measurements*

P. Wilson, G. Koepke, J. Ladbury, C. L. Holloway

National Institute of Standards and Technology
325 Broadway, Boulder, Colorado 80305

Abstract: This paper examines the use of total radiated power measurements, combined with theory-based directivity estimates, to generate accurate estimates for the maximum radiation and reception from a device. This approach may be a useful alternative to present test methods for emission and immunity as frequencies above 1 GHz become necessary for EMC standards. Radiation-pattern data for theory-based estimates, Monte Carlo simulations of an arbitrary device, and measurements on a sample device are presented, and good data agreement is demonstrated.

1. Introduction

Electronic devices are usually located in complex electromagnetic environments such as office rooms, factory floors, aircraft hulls, and so forth. The goal of standardized radiated field emission and immunity measurements is to ensure EMC in these complex environments. Intuitively, we would expect that radiated field measurements would seek to replicate these complex environments. However, this is not the case for several reasons. First, real environments are simply too varied to be comprehensively simulated. Second, the need to compare and repeat measurements requires well-defined, invariant measurement environments. Thus, standardized EMC radiated field measurements are performed in noncomplex environments of low quality factor (Q), such as anechoic chambers and open area test sites (OATS).

Standardized emission and immunity measurements implicitly assume that the equipment under test (EUT) has a simple radiation and reception pattern (e.g., dipole-like). This implicit assumption means that only a few EUT orientations are needed to find a reasonable estimate for the EUT's maximum radiated and received field. However, as the EUT becomes large, when compared to a wavelength, the radiation and reception pattern becomes complicated, with sharp beams and deep nulls [1-4]. A few orientations will no longer suffice to obtain a reasonable estimate of the maximum radiated/received fields. Very meticulous rotational sampling routines must be used to accurately measure a complex pattern. However, performing measurements of a full antenna pattern is expensive and time consuming. Thus, such measurements are not suitable for routine EMC test purposes.

This paper discusses an alternative approach to radiated EMC measurements that is better suited to higher frequencies (complex radiation patterns) and complex environments (high Q). The basic differences are the substitution of radiated power measurements for the present field-at-a-distance measurements, the substitution of statistically-based EUT-directivity estimates for the present limited directivity measurements, and the substitution of statistically based estimates of complex environment Q for the present non-complex measurement environments. This basic approach is presently being explored in two IEC draft standards (61000-4-20: TEM Cells and 61000-4-21: Reverberation Chambers).

This paper is organized as follows. Sections 2 and 3 discuss how estimated directivity and Q values may be used to simplify EMC emission and immunity measurements. Section 4 briefly covers measurements of total radiated power in reverberation chambers (high-frequency approach) and TEM cells (low-frequency approach). Sections 5 and 6 indicate how directivity and Q may be estimated for an arbitrary EUT and volume, respectively. Section 7 briefly discusses how a room's decay constant can be used to determine whether that volume is low Q (direct path coupling is dominant) or high Q (resonances may be dominant). The test levels for an EUT should depend on its intended environment. Section 8 shows some simulations of an arbitrary EUT based on a random set of simple sources. Section 9 gives measured data for a pseudo-arbitrary EUT and compares these to theoretical estimates from Section 5 and the simulation model from Section 8. Section 10 gives some concluding remarks.

2. Radiated Emissions

EMC tests of radiated emissions seek to determine the maximum far-field radiated by the EUT. If the total radiated power P_{rad}^{eut} (total implies over all spatial directions for a defined bandwidth) and the maximum directivity D_{max} of an EUT are known, then the maximum far-zone electric field E_{max} at a distance r in free space is given by [5]

$$E_{max} = \frac{1}{r} \left(\frac{D_{max} \eta P_{rad}^{eut}}{4\pi} \right)^{1/2}, \quad (1)$$

where $\eta = 120\pi$ (Ω) is the free space intrinsic wave impedance. This expression may be rewritten as

$$\frac{r^2 E_{\max}^2}{\eta P_{\text{rad}}^{\text{eut}}} = \frac{D_{\max}}{4\pi}. \quad (2)$$

If D_{\max} can be estimated and $P_{\text{rad}}^{\text{eut}}$ is known (via measurement), then the maximum field can be estimated.

Equation (2) estimates the line-of-sight far field. If the EUT is located in a confined volume of high Q , then the maximum field level may depend on room resonances rather than line-of-sight coupling [6]. Examples would be a personal computer located in a highly metallic office space, or electronics located in the hull of an air or sea craft. A better check of emissions in high- Q environments would be to determine the maximum expected field as a function of the cavity's Q . One can show [7] that the average field E_0 in a cavity is related to the source power and Q via

$$E_0^2 = \frac{Q}{2\pi} \frac{\lambda}{V} \eta P_{\text{rad}}^{\text{eut}}, \quad (3)$$

where V is the cavity volume. Assuming that the real and imaginary parts of the electric field's rectangular-components are independent, and that each is normally distributed with zero mean and equal variance, then the probability-density function of the electric field's magnitude is a chi function with six degrees of freedom [7]. Based on this model, the expected value of the maximum received power as a function of the number of points (N) measured in the room [8] is related to the average received power in the room by

$$\langle P_{\text{rec,max}} \rangle \approx \langle P_{\text{rec}} \rangle (0.577 + \ln N), \quad (4)$$

where N is assumed to be large, $N \gg 1$. The same factor modifies the field density, yielding

$$\frac{\lambda^2 E_{\max}^2}{\eta P_{\text{rad}}^{\text{eut}}} \approx \frac{Q}{2\pi} \frac{\lambda^3}{V} (0.577 + \ln N). \quad (5)$$

If Q can be estimated and $P_{\text{rad}}^{\text{eut}}$ is known (via measurement), then the maximum field can be estimated. This result (5) has no upper bound. This follows from the assumptions that the field components are described by unbounded normal distributions and that they are uncorrelated at all points. Nearby points will be correlated. $\lambda/2$ is a good estimate of the correlation length [7]. If the cavity volume is partitioned into $\lambda/2$ -sized cells and we assign one measurement point per cell, the resulting N ($\approx 8V/\lambda^3$) gives a useful upper bound. Inserting this estimate for N into (5) yields

$$\frac{\lambda^2 E_{\max}^2}{\eta P_{\text{rad}}^{\text{eut}}} \approx \frac{Q}{2\pi} \frac{\lambda^3}{V} \left(0.577 + \ln \frac{8V}{\lambda^3} \right). \quad (6)$$

These maximum field estimates give us flexibility in setting acceptable emission levels for an EUT. In low- Q environments (large lossy volumes, residential), emission levels can be determined using directivity estimates. In high- Q environments (small reflecting volumes, commercial, military), emission levels can be determined using Q estimates. In both cases only the total power radiated by the EUT needs to be measured. Directivity and Q estimates are discussed in later sections.

The total-radiated-power method would be an alternative to the present CISPR 16 emission test method where, at each frequency, the EUT needs to be rotated (about its vertical axis) and the receiving antenna height scanned to determine the emission maximum. The present method also does not directly account for emissions outside the region defined by the EUT rotation and the receive antenna's height scan, unless the EUT is reoriented (not possible for gravity-sensitive devices).

3. Radiated Immunity

EMC immunity tests seek to determine whether a specific field level will cause interference to an EUT. If the EUT is tested over all directions at an average scalar power density E_0^2/η , and the maximum directivity D_{\max} is known, then the maximum received power $P_{\text{rec,max}}^{\text{eut}}$ is given by

$$P_{\text{rec,max}}^{\text{eut}} = A_{e,\max} \frac{E_0^2}{\eta} = \frac{\lambda^2}{4\pi} D_{\max} \frac{E_0^2}{\eta}, \quad (7)$$

where $A_{e,\max}$ is the maximum effective aperture. As with equation (2), equation (7) may be rewritten as

$$\frac{\eta P_{\text{rec,max}}^{\text{eut}}}{\lambda^2 E_0^2} = \frac{D_{\max}}{4\pi}. \quad (8)$$

If D_{\max} can be estimated and E_0 is known (via measurement) then the maximum received power can be determined.

In a high- Q cavity with a known radiative power source $P_{\text{rad}}^{\text{source}}$, the maximum received power can be estimated as

$$\frac{P_{\text{rec,max}}^{\text{eut}}}{P_{\text{rad}}^{\text{source}}} \approx \frac{D_{\max}}{4\pi} \frac{Q}{2\pi} \frac{\lambda^3}{V} (0.577 + \ln \frac{8V}{\lambda^3}). \quad (9)$$

This would be an alternative to the present IEC 61000-4-3 immunity test method where, at each frequency, the EUT is rotated to expose four sides for each of two electric field polarizations, vertical and horizontal. As will be seen in later

sections, at higher frequencies, where the EUT reception pattern may be quite complicated, four sample points may have a very low probability of determining the maximum power received by the EUT. Reception along the vertical axis direction is not tested, unless the EUT is reoriented (not possible for gravity-sensitive devices).

4. Total Radiated Power

The total radiated power over the measurement bandwidth may be efficiently determined using several methods. Two practical approaches are reverberation chambers at higher frequencies, and TEM cells at lower frequencies.

The reverberation chamber method is based on first calibrating the chamber by measuring the power received (P_{rec}^{cal}) from a known radiation source (P_{rad}^{cal}) over a sufficient number of paddle positions to determine a reliable average. The EUT is then substituted for the calibration source, and the received power (P_{rec}^{eut}) is measured over the same set of paddle positions. The total radiated power determined via [7] is then

$$\langle P_{rad}^{eut} \rangle = \frac{\langle P_{rad}^{cal} \rangle}{\langle P_{rec}^{cal} \rangle} \langle P_{rec}^{eut} \rangle, \quad (10)$$

where $\langle \rangle$ denotes average. The reverberation chamber method works well as long as the mode density in the chamber is sufficiently large to yield meaningful statistics. This requirement determines a lower frequency limit.

The basic TEM cell method assumes that the EUT is well represented by a set of electric and magnetic dipoles. This should be a valid assumption for $ka \leq 1$, where $k = 2\pi/\lambda$, λ (m) is the free space wavelength, and a (m) denotes the radius of the minimum sphere bounding the EUT. P_{rad}^{eut} may be determined from the measured voltages ($V_{rec,i}^{eut}$) for three orthogonal positions. The details may be found in [9].

5. Directivity Estimates

The maximum directivity D_{max} for an emitter that can be enclosed in a sphere of radius a can be derived from spherical wave theory [10-11]

$$D_{max} \approx \begin{cases} 3, & ka \leq 1 \\ (ka)^2 + 2ka, & ka > 1 \end{cases} \quad (13)$$

While D_{max} is a good upper bound for all emitters, including intentional high-gain antennas, it overestimates directivity for unintentional emitters of interest in EMC measurements. A better estimate for EMC purposes can be derived by assuming that the spherical-mode coefficients are independent random

variables [11]. The expected value for D_{max} based on this assumption is well estimated by

$$\langle D_{max} \rangle \approx \begin{cases} 1.55, & ka \leq 1 \\ \frac{1}{2} \left[0.577 + \ln(4(ka)^2 + 8ka) \right] + \frac{1}{8(ka)^2 + 16ka}, & ka > 1. \end{cases} \quad (14)$$

For $ka \gg 1$ this expression simplifies to

$$\langle D_{max} \rangle \approx 0.982 + \ln(ka), \quad ka \gg 1. \quad (15)$$

These results apply to directivity determined over the whole sphere. Similar results may be derived for the received power measured over a planar cut [11]. Again, assuming that spherical-mode coefficients are independent random variables, the expected value of the maximum to the mean received power over the cut can be estimated as

$$\frac{\langle P_{rec,max} \rangle}{\langle P_{rec} \rangle} \approx \begin{cases} 2.45, & ka \leq 1 \\ 0.577 + \ln(4ka) + 2 + \frac{1}{8ka + 4}, & ka > 1. \end{cases} \quad (16)$$

Although this expression doesn't estimate maximum directivity, as needed in Sections 2-3, it can be readily compared to measured and simulated planar-cut data, as done in Section 7. Good agreement in the simpler planar-cut case will lend validity to the use of (9) for maximum directivity estimates for a full sphere.

6. Quality Factor Estimates

Several estimates for the Q of rooms may be used [6-7]. For a room of volume V and surface area A , Q may be estimated from

$$Q \approx k \frac{V}{A \alpha}, \quad (17)$$

where α is the average of the room's surface-absorption coefficient over all angles of incidence angle β and all polarizations. For a room with highly conductive walls such that $\sigma_w/(\omega\epsilon_w) \gg 1$, where σ_w and ϵ_w are the wall's conductivity and permittivity respectively, this Q estimate reduces to [12]

$$Q \approx \frac{3V}{2\mu_r \delta A}, \quad (18)$$

where μ_r is the relative permeability of the wall ($\mu_r = \mu_w / \mu$), μ and μ_w are, respectively, the free space and wall permeabilities, and δ is the skin depth, $\delta \approx \sqrt{2/\omega\mu_w\sigma_w}$. These expressions for Q only account for wall losses. Additional loss mechanisms such as EUT loading, aperture

leakage, and the receive antenna's load dissipation may also be accounted for [7].

7. Line-of-Sight or Resonance Coupling

An EUT may be located in a low- Q , or open, environment where line-of-sight coupling or simple reflection paths may be dominant. Or it may be located in a high- Q , or closed, environment where chamber resonances are dominant. In deciding which environment is appropriate we need to consider the reflective properties of the space containing the EUT. One method toward characterizing volumes as direct-path dominant or resonant dominant is to examine the decay of the power in a room when excited by a pulsed source. It is shown in [6] that reverberation develops in a room after four to five characteristic room times t_c , where

$$t_c \approx \frac{8V}{cA}, \quad (19)$$

and c is the speed of light. Also in [6], it is shown that the field level in an office room with typical building materials may be very small after $5t_c$, due to the low reflections properties of the walls. Thus, for some office room situations a reverberant environment may not develop.

The model in [6] can be used to estimate whether an environment is reverberant or free-space in the following manner. The average field level in the room environment at $3t_c$ is estimated. If this field level is significantly smaller (three orders of magnitude) than the free-space line-of-sight field level, then the room can be approximated as a free-space environment. If not, assume it to be a reverberant environment.

8. Simulated Directivity

A simple model of an arbitrary EUT will be used for comparison to theoretical estimates. We assume that a set of isotropic point sources are randomly distributed about the surface of a sphere (θ, ϕ) of radius a . Each source has random magnitude I and phase α . All variables are uniformly distributed over their respective ranges:

$$\theta \in [0, \pi], \phi \in [0, 2\pi], I \in [0, 1], \alpha \in [0, 2\pi]. \quad (20)$$

The far-field received power from this source set [13] is proportional to

$$P_{rec}(\theta, \phi) = \left| \sum_{i=1}^N I_i e^{j(kr \cos \psi_i + \alpha_i)} \right|^2, \quad (21)$$

where $\cos \psi_i = \cos \theta \cos \theta_i + \sin \theta \sin \theta_i \cos(\phi - \phi_i)$, and (θ_i, ϕ_i) identifies the location of the i th source.

This model loosely simulates an enclosure with various electrically small surface sources due to apertures, seams, connectors, etc. Real EUT sources will have some directivity (e.g., dipole-like) and the pattern will be affected by the EUT housing. However, this simple model should demonstrate the basic directivity characteristics of a set of simple sources.

As an example, consider the following case. Assume an EUT diameter of 50 cm ($a = 0.25$), a set of 5 sources, and an upper frequency limit of 5 GHz ($ka \approx 26$). The above expression can be used to simulate the results from a planar cut (1° angular steps) for comparison to the estimate given by (16). The results for a sample simulation run are shown in Figures 1-3.

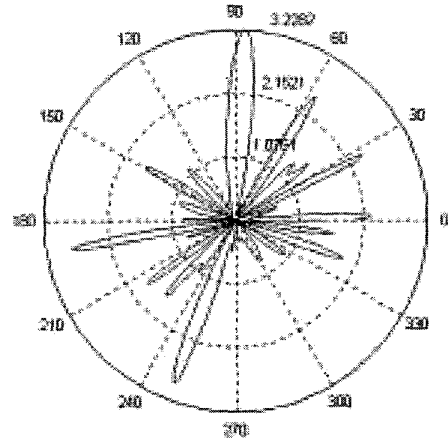


Figure 1. The radiation pattern (x-z axes plane) for a set of 5 arbitrary sources located on a sphere of radius 0.25 m, $ka = 26$.

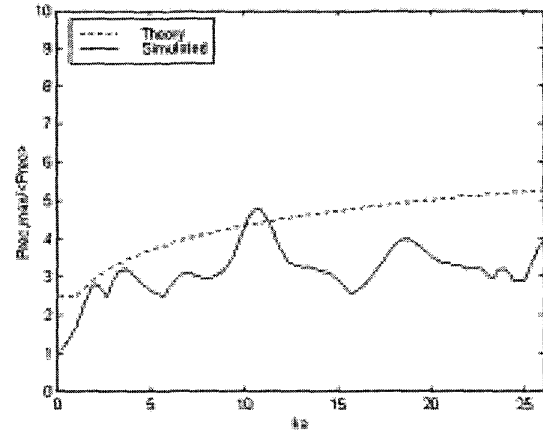


Figure 2. The estimated (theory) and simulated $P_{rec,max}/\langle P_{rec} \rangle$ ratio for the same source set as in Figure 1.

Figure 1 shows the radiation pattern at the highest frequency ($ka = 26$). The pattern shows multiple narrow lobes. Figure 2 shows the estimated and simulated maximum-to-mean received power ratio over the chosen planar cut. The simulation has some values above the estimate showing the statistical variation about the mean maximum.

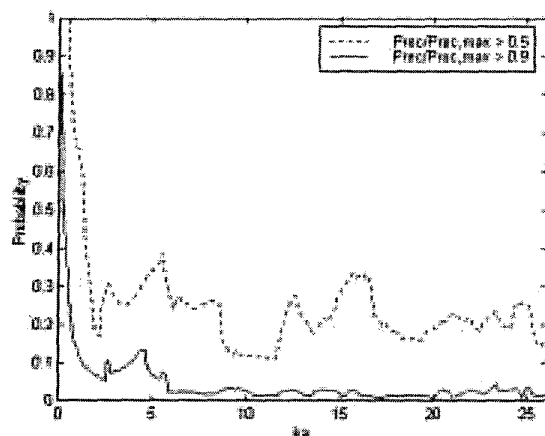


Figure 3. The probability that P_{rec} , at an arbitrary point on the planar cut, exceeds either 50 % or 90 % of $P_{rec, max}$.

Figure 3 shows the probability that P_{rec} , at an arbitrary point on the planar cut, exceeds either 50 % or 90 % of the received power maximum, $P_{rec, max}$. For $ka > 5$, the probability that an arbitrarily chosen point gives a P_{rec} value within 90 % of the maximum is significantly less than 10 %. This emphasizes that a few measurement points will not likely give a good indication of directivity once the EUT is electrically large.

We used the above parameters (5 sources, $a = 0.25$, $ka \approx 26$) in a 100-run Monte Carlo simulation to determine an average value for $P_{rec, max}/\langle P_{rec} \rangle$ that can be compared to the theory estimate (16). The results are shown in Figure 4. The figure shows that the theory gives a very conservative upper bound on average for the case of five sources. If we increase the number of sources to 50, then simulated maximum-to-mean received power more closely approaches the theoretical estimate, as shown in Figure 5.

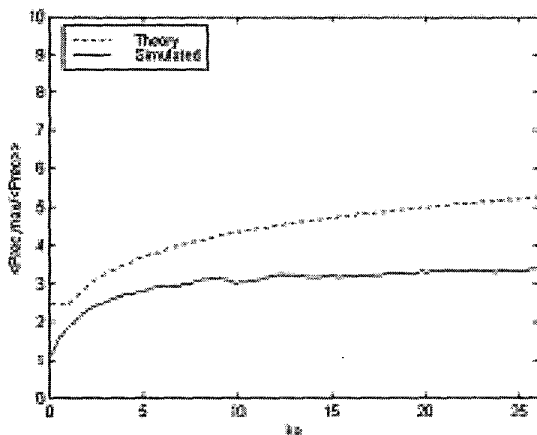


Figure 4. The theoretical and simulated $\langle P_{rec, max} \rangle / \langle P_{rec} \rangle$ ratio for 5 arbitrary isotropic sources randomly placed on a 0.25 m radius sphere using a Monte Carlo run of 100 simulations.

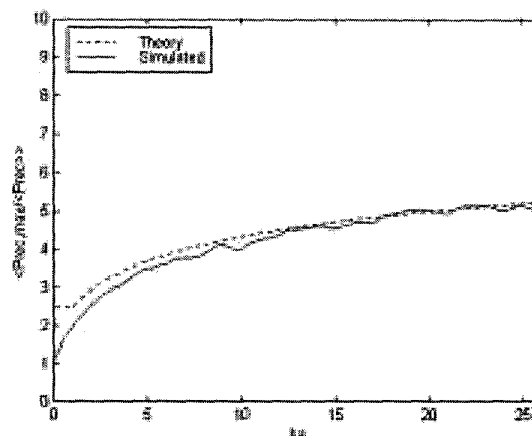


Figure 5. The theoretical and simulated $\langle P_{rec, max} \rangle / \langle P_{rec} \rangle$ ratio for 50 arbitrary isotropic sources randomly placed on a 0.25 m radius sphere using a Monte Carlo run of 100 simulations.

9. Measured Directivity Example

A simple EUT was constructed to perform pattern and directivity measurements. The EUT consisted of a rectangular metallic box (0.73 x 0.93 x 0.103 m) with five 1.5 cm holes randomly placed on each face. A horn antenna excited the box interior. The horn antenna was driven by a signal generator connected via a coaxial cable to a connector on a face of the box. Planar cuts were measured from 2 GHz to 4 GHz in 40 MHz steps. Figure 6 shows a representative planar cut for the 30-hole EUT at 2 GHz. Planar cuts at higher frequencies show even narrower lobes.

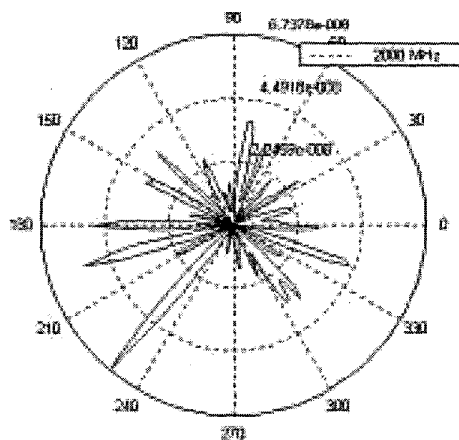


Figure 6. Measured 30-hole EUT radiation pattern at 2.0 GHz.

The 30-hole EUT has an internal paddle to change the distribution of the aperture excitation. This allows us to generate statistics as if different EUTs were being measured. Figure 7 shows the average results similar to Figures 4-5, theory and measured, for the max-to-mean received power based on 48 random pattern measurements. The measured data

closely approach the theoretical estimate, much as in Figure 6 where the source number was also high. We can simulate this EUT using 15 random sources (we assume that the metallic case mostly shields the backside apertures) and a sphere with a radius of 0.784 m (based on the EUT diagonal). Figure 9 also shows the result for a 48-run Monte Carlo simulation based on these parameters. The simulation well mimics the characteristics of the measured data.

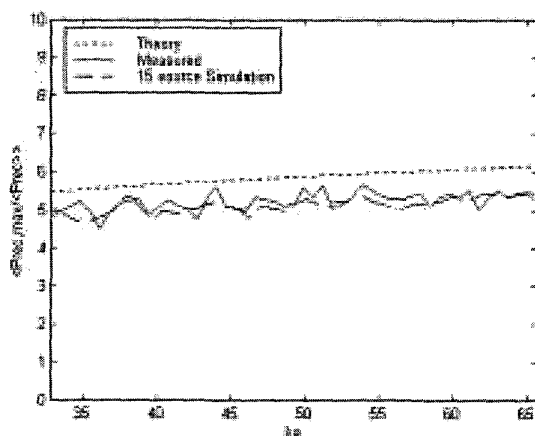


Figure 7. The estimated (theory), measured, and simulated (15 sources) $P_{rec,max}/\langle P_{rec} \rangle$ ratio for the 30-hole EUT.

10. Conclusion

The good agreement between theory, measurement, and simulation validates the basic statistical approach used here. Thus, we can use (14) to estimate the maximum directivity of the 30-hole EUT. If the 30-hole EUT total radiated power has been measured (e.g., in a reverberation chamber or TEM cell), then equations (2) and (5) can be used to estimate the maximum field at a given distance. If the incident power density on the 30-hole EUT is known, then equations (7) and (9) can be used to estimate the maximum received power. A continuing measurement program is underway to verify these statements. If the accuracy of this approach can be well established, then the method would form a good basis for future EMC standards at higher frequencies where the complexity of the EUT pattern makes present approaches either too time consuming (too many measurement points) or inaccurate (near-maximum direction not measured). In addition, the real EUT application environment, either open or resonant, could be considered when setting standard pass/fail levels.

References

[1] L. Jansson and M. Bäckström, "Directivity of equipment and its effect on testing in mode-stirred and anechoic chambers," Proc. 1999 IEEE Intl. Symp. on EMC (Seattle, WA), pp. 17-22, Aug. 1999.

[2] M. Johnson, M. Hatfield, M. Slocum, and G. Freyer, "Complications in correlatability between test techniques due to directional emissions patterns," Proc. 1999 IEEE Intl. Symp. on EMC (Seattle, WA), pp. 776-779, Aug. 1999.

[3] G. Freyer and M. Bäckström, "Comparison of anechoic & reverberation chamber coupling data as a function of directivity pattern," Proc. 2000 IEEE Intl. Symp. on EMC (Wash., DC), pp. 615-620, Aug. 2000.

[4] S. Clay, "Improving the correlation between OATS, RF anechoic room and GTEM radiated emissions measurements for directional radiators at frequencies between approximately 150 MHz and 10 GHz," Proc. 1999 IEEE Intl. Symp. on EMC (Seattle, WA), pp. 1119-1124, Aug. 1999.

[5] D. Hill, D. Camell, K. Cavcey, and G. Koepke, "Radiated emissions and immunity of microstrip transmission lines: theory and reverberation chamber measurements," IEEE Trans. Electromag. Compat., vol. 38, no. 2, pp. 165-172, May 1996.

[6] C. Holloway, M. Cotton, and P. McKenna, "A model for the predicting the power delay profile characteristics inside a room," IEEE Trans. Vehicular Tech., vol. 48, no. 4, pp. 1110-1120, July 1999.

[7] D. Hill, "Electromagnetic theory of reverberation chambers," NIST Technical Note 1506, Dec. 1998.

[8] J. Ladbury, T. Lehman, and G. Koepke, "Reverberation chamber distributions 1: maximum received power," draft NIST Technical Note.

[9] P. Wilson, "On correlating TEM cell and OATS emission measurements," IEEE Trans. Electromag. Compat., vol. 37, no. 1, pp. 1-16, Feb. 1995.

[10] J. Hansen, Spherical Near-Field Antenna Measurements, Peter Peregrinus: London, 1988.

[11] G. Koepke, D. Hill, and J. Ladbury, "Directivity of the test device in EMC measurements," Proc. 2000 IEEE Intl. Symp. on EMC (Wash., DC), pp. 535-539, Aug. 2000.

[12] D. Hill, "A reflection coefficient derivation for the Q of a reverberation chamber," IEEE Trans. Electromag. Compat., vol. 38, no. 4, pp. 591-592, Nov. 1996.

[13] M. Ma, Theory and Application of Antenna Arrays, Wiley & Sons, New York, 1974.